The Optical Gravitational Lensing Experiment. Cepheids in the Magellanic Clouds. IV. Catalog of Cepheids from the Large Magellanic Cloud*

A. Udalski[1], I. Soszyński[1], M. Szymański[1], M. Kubiak[1], G. Pietrzyński[1], P. Woźniak[2], and K. Żebruń[1]

[1]Warsaw University Observatory, Al. Ujazdowskie 4, 00-478 Warszawa, Poland
e-mail: (udalski,soszynsk,msz,mk,pietrzyn,zebrun)@sirius.astrouw.edu.pl
[2] Princeton University Observatory, Princeton, NJ 08544-1001, USA
e-mail: wozniak@astro.princeton.edu

ABSTRACT

We present the Catalog of Cepheids from the LMC. The Catalog contains 1333 objects detected in the 4.5 square degree area of central parts of the LMC. About $3.4 \cdot 10^5$ *BVI* measurements of these stars were collected during the OGLE-II microlensing survey. The Catalog data include period, *BVI* photometry, astrometry, and R_{21},ϕ_{21} parameters of the Fourier decomposition of *I*-band light curve.

The vast majority of objects from the Catalog are the classical Cepheids pulsating in the fundamental or first overtone mode. The remaining objects include Population II Cepheids and red giants with pulsation-like light curves.

Tests of completeness performed in overlapping parts of adjacent fields indicate that completeness of the Catalog is very high: $> 96\%$. Statistics and distributions of basic parameters of Cepheids are also presented.

Finally, we show the light curves of three eclipsing systems containing Cepheid detected among objects of the Catalog.

All presented data, including individual *BVI* observations are available from the OGLE Internet archive.

1 Introduction

Cepheids were among the first variable stars discovered by astronomers – the prototype of the class, δ Cep, and η Aql were found to be varying in brightness by J. Goodricke and E. Pigott, respectively, in 1784. The great career of these objects begun at the beginning of 20th century when their

*Based on observations obtained with the 1.3 m Warsaw telescope at the Las Campanas Observatory of the Carnegie Institution of Washington.

famous Period–Luminosity relation was discovered in the Small Magellanic Cloud by Leavitt (1912). Cepheids became one of the most important standard candles used for distance determination in the Universe, although the calibration of the Period–Luminosity relation is still a topic of lively debate. Proper calibration is of great importance because Cepheids are now routinely discovered in galaxies to about 25 Mpc with the HST instruments. Thus, the Cepheid based distance scale is one of the most important steps in the distance scale ladder.

Cepheids are relatively well understood pulsating stars. Their role in the modern astrophysics is hard to be overestimated. Beside the Period–Luminosity relation these objects are the ideal laboratory for testing the stellar structure, theory of stellar evolution etc. Therefore it is crucial to have at hand a large sample of these stars with good quality observational data so the theoretical work could be verified.

Although many Cepheids were discovered in the Galaxy their observational data are very inhomogeneous, taken by different observers with different instruments. Two nearby galaxies – the Magellanic Clouds – are potentially much better hosts of these objects. Both Large and Small Magellanic Clouds are known to contain many Cepheids. Additional advantage of Cepheids from these galaxies is that they are located at approximately the same distance what makes analyses of their properties much simpler.

Unfortunately both Magellanic Clouds have been neglected photometrically for years – the vast majority of known Cepheids in the Magellanic Clouds were observed with old photographic or photoelectric techniques giving an order of magnitude worse quality than the modern CCD-based techniques. Situation has significantly changed in 1990s when large microlensing surveys begun regular monitoring of the Magellanic Clouds for microlensing events. Photometry of millions stars in both Magellanic Clouds is a natural by-product of these surveys and for the first time good quality light curves of the Magellanic Cloud Cepheids could be obtained. Both MACHO and EROS microlensing surveys reported discovery of many Cepheids and presented observations of these stars in the LMC and/or SMC (Alcock *et al.* 1995, Alcock *et al.* 1999, Sasselov *et al.* 1997, Bauer *et al.* 1999). Unfortunately, all these data were taken with non-standard photometric bands.

The Magellanic Clouds were added to the list of objects observed by the Optical Gravitational Lensing Experiment (OGLE) at the beginning of the second phase of the survey in January 1997. Since then both Magellanic Clouds are monitored regularly, practically on every clear night. Observations are made through the BVI filters very closely reproducing the standard

BVI system. After more than two years of observations the photometric databases are complete enough so the search for variable stars could be performed. Large samples of Cepheids were extracted from databases of both Magellanic Cloud fields.

In the previous papers of this series we presented analysis of double-mode Cepheids in the SMC (Udalski *et al.* 1999a), discovery of 13 Cepheids in the SMC – candidates for objects pulsating in the second overtone mode (Udalski *et al.* 1999b) and analysis of the Period–Luminosity and Period–Luminosity–Color relations of huge samples of Cepheids from the LMC and SMC (Udalski *et al.* 1999c). In this paper we present first of two Catalogs of Cepheids from the Magellanic Clouds – the Catalog of Cepheids from the LMC. Similar Catalog of about 2300 Cepheids from the SMC will follow.

The Catalog of Cepheids from the LMC contains 1333 objects. They come from the 4.5 square degree area of central parts of the LMC. The vast majority of them are the classical Cepheids. Other stars include a sample of Population II Cepheids and a sample of red giant objects which variability resembles pulsation-like light curves. We do not include additional sample of about 70 double-mode Cepheids detected in the LMC – these objects will be described in a separate paper similar to double-mode Cepheids from the SMC (Udalski *et al.* 1999a).

We also present statistics and distributions of basic parameters of the LMC Cepheids like location in the LMC, periods, colors and parameters of the Fourier decomposition of light curve. Finally, we point attention to three Cepheids in the eclipsing systems which could potentially provide precise data on sizes and masses of their components.

The large and homogeneous sample of Cepheids presented in this paper with high quality photometry and high completeness can be used for many projects concerning these stars. Therefore we decided to make the data public – all data presented in this paper, including individual *BVI*-band observations and finding charts are available from the OGLE Internet archive.

2 Observations

All observations presented in this paper were carried out during the second phase of the OGLE experiment with the 1.3-m Warsaw telescope at the Las Campanas Observatory, Chile, which is operated by the Carnegie Institution of Washington. The telescope was equipped with the "first generation"

camera with a SITe 2048×2048 CCD detector working in drift-scan mode. The pixel size was 24 μm giving the 0.417 arcsec/pixel scale. Observations of the LMC were performed in the "slow" reading mode of CCD detector with the gain 3.8 e^-/ADU and readout noise of about 5.4 e^-. Details of the instrumentation setup can be found in Udalski, Kubiak and Szymański (1997).

T a b l e 1

Equatorial coordinates of the OGLE-II LMC fields

Field	RA (J2000)	DEC (J2000)
LMC_SC1	$5^h33^m49^s$	$-70°06'10''$
LMC_SC2	$5^h31^m17^s$	$-69°51'55''$
LMC_SC3	$5^h28^m48^s$	$-69°48'05''$
LMC_SC4	$5^h26^m18^s$	$-69°48'05''$
LMC_SC5	$5^h23^m48^s$	$-69°41'05''$
LMC_SC6	$5^h21^m18^s$	$-69°37'10''$
LMC_SC7	$5^h18^m48^s$	$-69°24'10''$
LMC_SC8	$5^h16^m18^s$	$-69°19'15''$
LMC_SC9	$5^h13^m48^s$	$-69°14'05''$
LMC_SC10	$5^h11^m16^s$	$-69°09'15''$
LMC_SC11	$5^h08^m41^s$	$-69°10'05''$
LMC_SC12	$5^h06^m16^s$	$-69°38'20''$
LMC_SC13	$5^h06^m14^s$	$-68°43'30''$
LMC_SC14	$5^h03^m49^s$	$-69°04'45''$
LMC_SC15	$5^h01^m17^s$	$-69°04'45''$
LMC_SC16	$5^h36^m18^s$	$-70°09'40''$
LMC_SC17	$5^h38^m48^s$	$-70°16'45''$
LMC_SC18	$5^h41^m18^s$	$-70°24'50''$
LMC_SC19	$5^h43^m48^s$	$-70°34'45''$
LMC_SC20	$5^h46^m18^s$	$-70°44'50''$
LMC_SC21	$5^h21^m14^s$	$-70°33'20''$

Observations of the LMC started on January 6, 1997. 11 driftscan fields covering 14.2×57 arcmins in the sky were observed during the first months of 1997. Additional 10 fields were added in October 1997 increasing the total observed area of the LMC to about 4.5 square degree. Because the microlensing search is planned to last for several years, observations of selected fields will be continued during the following seasons. In this paper we

present data collected up to June 1999.

Observations were obtained in the standard BVI-bands with majority of measurements made in the I-band. The effective exposure time was 125, 174 and 237 seconds for the I, V and B-band, respectively. The instrumental system closely resembles the standard BVI one – the color coefficients of transformation ($a \cdot CI$; a – color coefficient, CI – color index: $B-V$ for B and $V-I$ for VI filters) are equal to -0.041, $+0.004$ and $+0.032$ for the B, V and I-band, respectively.

Due to microlensing search observing strategy the vast majority of observations were done through the I-band filter (about $120-360$ epochs depending on the field) while images on about $15-40$ epochs were collected in the BV-bands. The B-band photometry is at the writing of this paper less complete than VI photometry – reductions of only 40% of fields were finished. For the remaining fields only VI photometry was available. B-band photometry of these fields will be completed after the next observing season.

Collected images were reduced with the standard OGLE data pipeline. Quality of data is similar to the photometric data of the SMC described in Udalski *et al.* (1998b). In particular, accuracy of absolute photometry zero points is about $0.01-0.02$ in all BVI-bands. More details on the LMC photometric data will be presented with release of the photometric maps of the LMC in the near future.

Table 1 lists equatorial coordinates of center of each field and its acronym. Fig. 1 shows the Digitized Sky Survey image of the LMC with contours of the observed fields.

3 Selection of Cepheids

The search for variable objects in the LMC fields was performed using observations in the I-band in which most observations were obtained. Typically about 120–360 epochs were available for each analyzed object with the lower limit set to 50. The mean I-band magnitude of analyzed objects was limited to $I < 19.5$ mag. Candidates for variable stars were selected based on comparison of the standard deviation of all individual measurements of a star with typical standard deviation for stars of similar brightness. Light curves of selected candidates were then searched for periodicity using the AoV algorithm (Schwarzenberg-Czerny 1989). The period search was limited to the range of 0.1–100 days. Accuracy of periods is about $7 \cdot 10^{-5} \cdot P$.

Candidates for Cepheids were selected from the entire sample of vari-

Fig. 1. OGLE-II fields in the LMC. Dots indicate positions of Cepheids from the Catalog. North is up and East to the left in the Digitized Sky Survey image of the LMC.

able stars based on visual inspection of the light curves and location in the color-magnitude diagram (CMD) within the area limited by $I<18.5$ mag and $0.25<(V-I)<1.3$ mag. Several objects located outside this region (*e.g.*, highly reddened Cepheids) and objects with no color information but with evident Cepheid-type light curves were also included to this sample. In total more than 1500 Cepheid candidates were found in the 4.5 square degree area of the LMC center.

Each of the analyzed LMC fields overlaps with neighboring fields for calibration purposes. Therefore several dozen Cepheids located in the overlapping regions were detected twice. We decided not to remove them from the final list of objects because their measurements are independent in both fields and can be used for testing quality of data, completeness of the sample etc. 105 such objects were detected and we provide cross-reference list to identify them.

4 Basic Parameters of Candidates

4.1 Intensity Mean Photometry

For each object which passed our selection criteria we derived the BVI intensity mean photometry by integrating the light curve converted to intensity units. It was approximated by the Fourier series of fifth order. Result was converted back to the magnitude scale. Accuracy of the mean I-band photometry is about $0.001 - 0.005$ mag and somewhat worse (about 0.01 mag) for poorer sampled BV-bands.

Full BVI photometry is available only for eight fields: LMC_SC1–LMC_SC8. For the remaining fields the B-band databases are not complete enough for precise determination of the mean brightness. Photometry of these fields will be completed after the next observing season of the LMC.

For each object we also determined the extinction insensitive index W_I (called also Wesenheit index, Madore and Freedman 1991):

$$W_I = I - 1.55 * (V - I) \tag{1}$$

The coefficient 1.55 in Eq. 1 corresponds to the coefficient resulting from standard interstellar extinction curve dependence of the I-band extinction on $E(V-I)$ reddening (*e.g.*, Schlegel, Finkbeiner and Davis 1998). It is easy to show that the values of W_I are the same when derived from observed or extinction free magnitudes, provided that extinction to the object is not too high so it can be approximated with a linear function of color.

4.2 Interstellar Reddening

Determination of the interstellar reddening to the LMC Cepheids has an important role in analyses of these objects, distance determination etc. It is well known that the reddening in the LMC is clumpy and variable (Harris, Zaritsky and Thompson 1998), therefore applying the mean reddening value to all objects is generally not justified.

With large photometric databases of millions stars we are in position to determine the average reddening in many lines-of-sight within the LMC. Unfortunately, we do not have U-band photometry which would allow to derive the reddening from young, hot OB stars. Therefore we used for this purpose much older but much more numerous red clump stars. It should be noted, however, that Cepheid population can be distributed in the LMC somewhat differently than red clump stars and OB-stars determination could

be more appropriate for Cepheids. On the other hand the differences should not be large for the LMC seen almost face-on.

We used red clump stars for mapping the fluctuations of mean reddening in our observed fields treating their mean *I*-band magnitude as the reference brightness. It was shown to be independent on age of these stars in the wide range of $2-10$ Gyr, and it is only slightly dependent on metallicity (Udalski 1998a,b). The latter correction is not important in this case because of practically homogeneous environment of field stars in the LMC (Bica *et al.* 1998). Thus, the mean brightness of red clump stars can be a very good reference of brightness for monitoring extinction. Similar method was used by Stanek (1996) for determination of extinction map of Baade's Window in the Galactic bulge.

The reddening in the LMC was determined in 84 lines-of-sight. We divided each of our 21 2048×8192 pixel fields to four 2048×2048 pixel subfields (subfield 1: $0<y<2048$, etc.). In each of the subfields we determined the mean observed *I*-band magnitude of red clump stars with technique identical to that described in Udalski *et al.* (1998a). Differences of the observed *I*-band magnitudes were assumed as differences of the mean A_I extinction. We converted differences of A_I extinction to differences of $E(B-V)$ reddening assuming the standard extinction curve: $E(B-V)=A_I/1.96$ (Schlegel *et al.* 1998).

The zero points of our reddening map were derived based on previous determinations in three lines-of-sight, two of them using OB-stars. These determinations included determination of reddening around two LMC star clusters: NGC1850 ($E(B-V)=0.15\pm0.05$ mag, based on *UBV* photometry, Lee 1995) and NGC1835 ($E(B-V)=0.13\pm0.03$ mag, based on colors of RR Lyr stars, Walker 1993) and determination based on OB-stars in the field of the eclipsing variable star HV2274 (Udalski *et al.* 1998c). All these zero points were consistent with our map to within a few thousands of magnitude.

We also checked the absolute calibration of our map comparing the observed *I*-band magnitude of red clump stars with extinction free magnitude determined from a few star clusters in the halo of the LMC (Udalski 1998b). We additionally checked the value of extinction free magnitude of red clump stars in the LMC by its new determination from the field stars around the same clusters. Resulting value was consistent to within 0.01 mag with star cluster red clump determination. The calibration *via* extinction free magnitude of red clump stars gave somewhat larger zero point of the $E(B-V)$ reddening – by about 0.02 mag which we adopt as the error of our map. The final $E(B-V)$ reddening in 84 lines-of-sight in the LMC is listed in Table 2.

T a b l e 2

$E(B-V)$ reddening in the LMC fields.

Field	Subfield 1 $E(B-V)$	Subfield 2 $E(B-V)$	Subfield 3 $E(B-V)$	Subfield 4 $E(B-V)$
LMC_SC1	0.117	0.152	0.147	0.163
LMC_SC2	0.121	0.121	0.150	0.131
LMC_SC3	0.134	0.120	0.123	0.117
LMC_SC4	0.130	0.120	0.105	0.118
LMC_SC5	0.130	0.115	0.108	0.133
LMC_SC6	0.138	0.125	0.107	0.123
LMC_SC7	0.143	0.138	0.142	0.146
LMC_SC8	0.131	0.133	0.136	0.142
LMC_SC9	0.143	0.165	0.156	0.149
LMC_SC10	0.156	0.147	0.146	0.132
LMC_SC11	0.147	0.154	0.150	0.152
LMC_SC12	0.152	0.146	0.127	0.139
LMC_SC13	0.154	0.129	0.135	0.130
LMC_SC14	0.124	0.142	0.138	0.127
LMC_SC15	0.145	0.125	0.147	0.126
LMC_SC16	0.135	0.148	0.185	0.181
LMC_SC17	0.171	0.193	0.175	0.201
LMC_SC18	0.182	0.178	0.173	0.170
LMC_SC19	0.153	0.153	0.187	0.167
LMC_SC20	0.132	0.137	0.142	0.163
LMC_SC21	0.133	0.152	0.145	0.146

Interstellar extinction in the BVI bands was calculated using the standard extinction curve coefficients (*e.g.*, Schlegel *et al.* 1998):

$$A_B = 4.32 \cdot E(B-V)$$
$$A_V = 3.24 \cdot E(B-V)$$
$$A_I = 1.96 \cdot E(B-V)$$

4.3 Astrometry

Equatorial coordinates of all candidates were calculated based on transformation derived with the Digitized Sky Survey images. Details of procedure are described in Udalski *et al.* (1998b). About $2800-7400$ stars common in

OGLE and DSS images (depending on stellar density of the field) were used for transformation. Internal accuracy of the equatorial coordinates is about 0.15 arcsec with possible systematic errors of the DSS coordinate system up to 0.7 arcsec.

4.4 Fourier Parameters of Light Curve Decomposition

For each object we derived Fourier parameters $R_{21}=A_2/A_1$ and $\phi_{21}=\phi_2-2\phi_1$ of the Fourier series decomposition of *I*-band light curve. A_i and ϕ_i are the amplitudes and phases of $(i-1)$ harmonic of the Fourier decomposition of light curve. Parameters R_{21} and ϕ_{21} are often used for analyses of pulsating variable stars and for discrimination between objects pulsating in different modes.

We fitted the fifth order Fourier series to the magnitude scale *I*-band light curve. In the case of objects with almost sinusoidal light curve for which the first harmonic amplitude and phase were not statistically significant, $R_{21}=0$ and ϕ_{21} is not defined.

4.5 Classification

Based on the Period-Luminosity $(P-L)$ diagram constructed for the extinction insensitive index W_I we divided all objects into four groups: classical Cepheids pulsating in the fundamental mode (FU), classical Cepheids pulsating in the first overtone mode (FO), objects brighter than FO mode Cepheids (BR) and objects fainter than FU mode Cepheids (FA). Fig. 2 presents $P-L$ diagram for the W_I index with boundaries of these four regions.

Due to very good accuracy of photometry and features of the W_I index, which removes simultaneously effects of extinction and color dependence of the Cepheid $P-L$ relation, the separation between the FU and FO Cepheids is remarkable. Nevertheless, we also checked location of all selected FU and FO Cepheids in the R_{21} and ϕ_{21} *vs.* $\log P$ diagrams. It is well known that such diagrams allow to separate between the FU and FO mode pulsators (*cf.* Alcock *et al.* 1999, Udalski *et al.* 1999a). Sequences for FU and FO Cepheids in both diagrams, in particular R_{21} *vs.* $\log P$, are well separated and in most cases classification is straightforward. However, in a few period ranges the sequences almost overlap (for $0.6<\log P<0.8$ in the R_{21} *vs.* $\log P$ diagram and $0.2<\log P<0.4$ and $\log P\approx 0.75$ in the ϕ_{21} *vs.* $\log P$ diagram). Therefore we checked light curves of all objects located in these regions

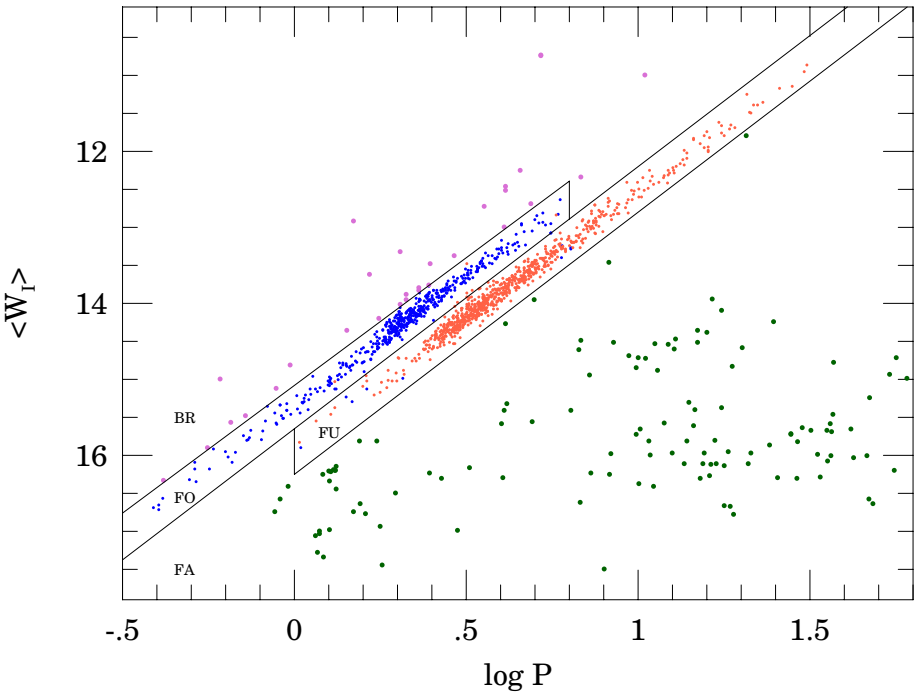

Fig. 2. Period-Luminosity relation for extinction insensitive index W_I. Contours divide the diagram into sections where fundamental (FU) and first overtone mode (FO) classical Cepheids are found. Section denoted by BR indicates region where objects were classified as brighter than FO Cepheids and by FA – as fainter than FU Cepheids. Small dots mark positions of objects finally classified as FU and FO classical Cepheids (light and dark dots, respectively). Larger dots – BR (light dots) and FA (dark dots) objects.

to confirm classification indicated by position in the $P-L$ diagram. Also all objects located in opposite mode sequences than indicated from $P-L$ position were inspected. In about 20 cases the classification was changed. In eight cases those were FU objects blended with other stars and therefore shifted to FO Cepheids in the $P-L$ diagram. In eleven cases – FO mode stars shifted to FU objects in the P–L diagram of the W_I index because of high reddening, blends with blue stars etc. Fig. 3 presents the final R_{21} *vs.* $\log P$ and ϕ_{21} *vs.* $\log P$ diagrams for all objects classified as FU and FO mode classical Cepheids.

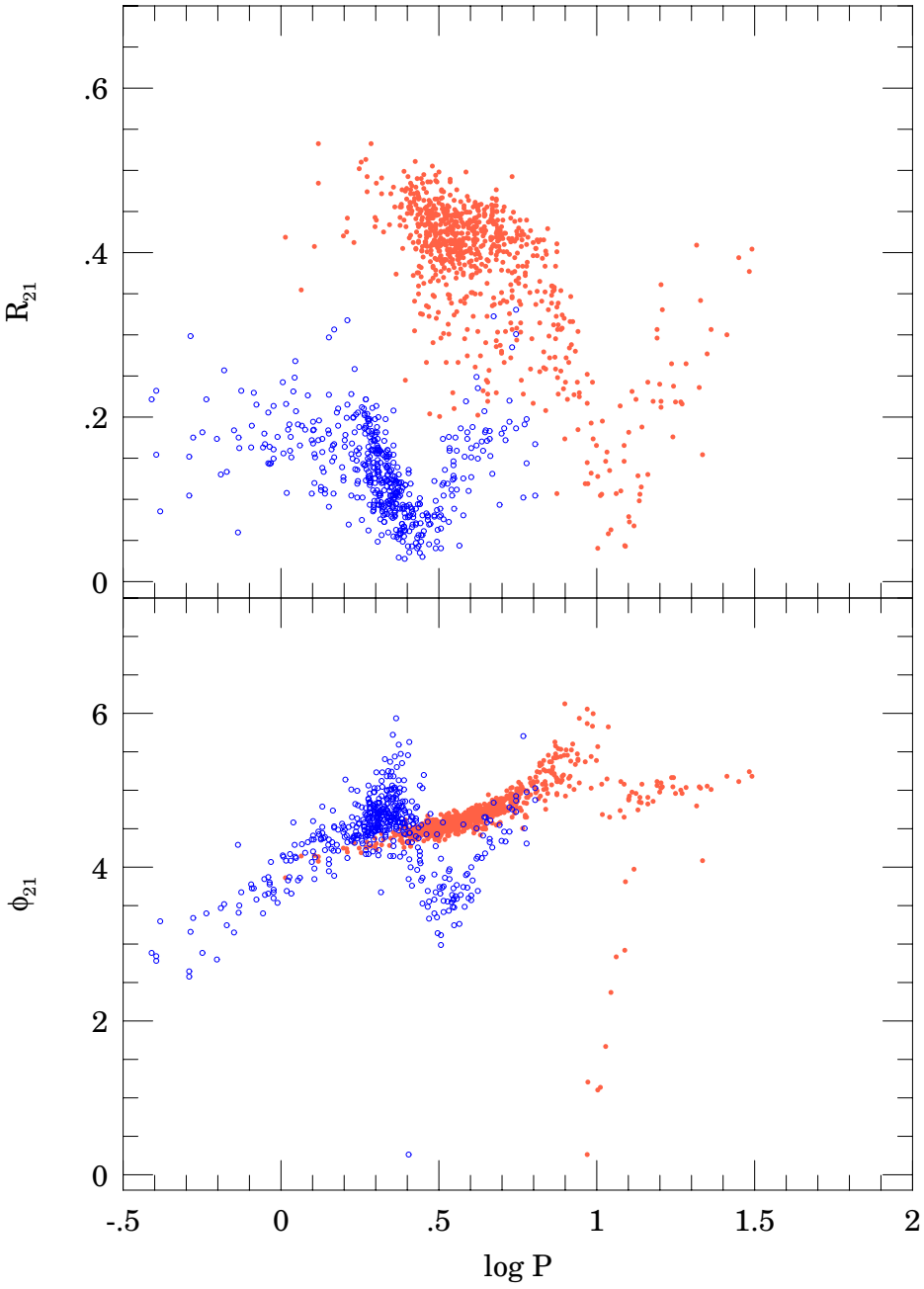

Fig. 3. R_{21} and ϕ_{21} *vs.* $\log P$ diagrams for single-mode classical Cepheids from the LMC. Dark open circles indicate positions of first overtone Cepheids while light dots positions of fundamental mode pulsators.

5 Catalog of Cepheids from the LMC

1402 objects passed our selection criteria described in Section 3. Among candidates for Cepheids in the LMC a subsample of double-mode classical Cepheids containing about 70 objects was extracted. These objects will be presented in a separate paper of this series. The remaining Cepheid candidates are listed in Table 3.

The first column of Table 3 is the star identification: *field_name star_number*. In the next columns the equatorial coordinates, RA and DEC (J2000), period in days and moment of the zero phase corresponding to maximum light are given. Then follow intensity mean IVB photometry supplemented by extinction insensitive index W_I and the mean interstellar reddening in object direction. In the next two columns Fourier parameters, R_{21} and ϕ_{21}, of the light curve decomposition are listed. Finally, in the last column classification of the object is provided.

Table 3 contains 1435 entries but only 1333 objects: 102 stars were detected twice – in overlapping parts of adjacent fields. Table 4 provides cross-identification of all such objects including for completeness three double-mode Cepheids not presented in this paper and not listed in Table 3.

The I-band light curves of all objects are presented in Appendices A–U. The ordinate is phase with 0.0 value corresponding to maximum light. Abscissa is the I-band magnitude. The light curve is repeated twice for clarity.

Finding charts ($60'' \times 60''$ part of the I-band image) are not presented in this paper but they are available in electronic form from the OGLE Internet archive (see below).

We did not attempt to cross-identify our objects with the ones known from literature. It would be a very difficult and time consuming task in so dense stellar fields without precise coordinates and finding charts. Because of very high completeness of the Catalog (see Section 6) – practically all Cepheids in the observed region of the LMC have been detected – and precise BVI photometry the OGLE catalog is likely to supersede much of the previous works. However, if necessary, cross-identification with selected objects can be done with precise coordinates and finding charts provided with the Catalog.

One should remember about the limit of the Catalog on the brighter, *i.e.*, longer period object side because of saturation of the CCD detector used. This limit corresponds to objects with period longer than $\log P \approx 1.5$, *i.e.*, longer than about 30 days.

T a b l e 4

Cross-identification of stars detected in overlapping regions

LMC_SC1	275300	↔	LMC_SC16	11573		LMC_SC12	210606	↔	LMC_SC11	37982
LMC_SC1	290572	↔	LMC_SC16	26258		LMC_SC13	12	↔	LMC_SC12	51598
LMC_SC1	295698	↔	LMC_SC16	31555		LMC_SC13	203493	↔	LMC_SC12	210640
LMC_SC1	313151	↔	LMC_SC16	48261		LMC_SC14	216182	↔	LMC_SC12	47109
LMC_SC1	324986	↔	LMC_SC16	57446		LMC_SC14	252799	↔	LMC_SC13	35171
LMC_SC2	334104	↔	LMC_SC1	31577		LMC_SC15	181509	↔	LMC_SC14	11554
LMC_SC2	334077	↔	LMC_SC1	31612		LMC_SC16	211276	↔	LMC_SC17	11199
LMC_SC2	349919	↔	LMC_SC1	44657		LMC_SC16	214736	↔	LMC_SC17	15426
LMC_SC2	357856	↔	LMC_SC1	51886		LMC_SC16	218499	↔	LMC_SC17	19793
LMC_SC2	365487	↔	LMC_SC1	59277		LMC_SC16	222451	↔	LMC_SC17	24561
LMC_SC3	368185	↔	LMC_SC2	39166		LMC_SC16	222497	↔	LMC_SC17	24574
LMC_SC3	376576	↔	LMC_SC2	47348		LMC_SC16	222476	↔	LMC_SC17	24585
LMC_SC3	384972	↔	LMC_SC2	55470		LMC_SC16	230207	↔	LMC_SC17	33268
LMC_SC3	393065	↔	LMC_SC2	63342		LMC_SC16	230281	↔	LMC_SC17	33286
LMC_SC3	408692	↔	LMC_SC2	78855		LMC_SC16	230222	↔	LMC_SC17	33289
LMC_SC4	369748	↔	LMC_SC3	5709		LMC_SC16	230285	↔	LMC_SC17	33290
LMC_SC4	369698	↔	LMC_SC3	5715		LMC_SC16	230224	↔	LMC_SC17	33292
LMC_SC4	399359	↔	LMC_SC3	35233		LMC_SC16	230228	↔	LMC_SC17	33299
LMC_SC4	399429	↔	LMC_SC3	35297		LMC_SC16	230273	↔	LMC_SC17	33351
LMC_SC4	408738	↔	LMC_SC3	44256		LMC_SC16	230290	↔	LMC_SC17	33368
LMC_SC4	417847	↔	LMC_SC3	53226		LMC_SC16	240480	↔	LMC_SC17	45198
LMC_SC4	417864	↔	LMC_SC3	53242		LMC_SC16	240497	↔	LMC_SC17	45207
LMC_SC4	418294	↔	LMC_SC3	53702		LMC_SC16	240460	↔	LMC_SC17	45218
LMC_SC5	343036	↔	LMC_SC4	13514		LMC_SC16	245458	↔	LMC_SC17	50018
LMC_SC5	424993	↔	LMC_SC4	98151		LMC_SC16	245478	↔	LMC_SC17	50024
LMC_SC6	356421	↔	LMC_SC21	193117		LMC_SC16	253780	↔	LMC_SC17	59761
LMC_SC6	356421	↔	LMC_SC5	6197		LMC_SC16	253794	↔	LMC_SC17	59808
LMC_SC6	369970	↔	LMC_SC5	19786		LMC_SC17	189196	↔	LMC_SC18	6114
LMC_SC6	369993	↔	LMC_SC5	19806		LMC_SC17	197292	↔	LMC_SC18	17714
LMC_SC6	377026	↔	LMC_SC5	26913		LMC_SC17	200401	↔	LMC_SC18	17724
LMC_SC6	404601	↔	LMC_SC5	58244		LMC_SC17	200430	↔	LMC_SC18	20948
LMC_SC6	405017	↔	LMC_SC5	67261		LMC_SC17	203767	↔	LMC_SC18	25000
LMC_SC6	422324	↔	LMC_SC5	75989		LMC_SC17	207480	↔	LMC_SC18	25015
LMC_SC7	356873	↔	LMC_SC6	27321		LMC_SC17	207506	↔	LMC_SC18	25041
LMC_SC7	372083	↔	LMC_SC6	40971		LMC_SC17	211310	↔	LMC_SC18	29237
LMC_SC7	380269	↔	LMC_SC6	49297		LMC_SC17	214843	↔	LMC_SC18	33576
LMC_SC7	415723	↔	LMC_SC6	85035		LMC_SC17	214859	↔	LMC_SC18	33591
LMC_SC7	425296	↔	LMC_SC6	86027		LMC_SC17	214860	↔	LMC_SC18	33594
LMC_SC7	432869	↔	LMC_SC6	102424		LMC_SC17	224169	↔	LMC_SC18	45433
LMC_SC7	440072	↔	LMC_SC6	102475		LMC_SC18	174802	↔	LMC_SC19	18878
LMC_SC7	447509	↔	LMC_SC6	118107		LMC_SC18	188926	↔	LMC_SC19	38257
LMC_SC8	312191	↔	LMC_SC7	55965		LMC_SC18	195674	↔	LMC_SC19	44947
LMC_SC8	326025	↔	LMC_SC7	79610		LMC_SC18	199069	↔	LMC_SC19	48659
LMC_SC8	337497	↔	LMC_SC7	86332		LMC_SC18	202349	↔	LMC_SC19	48662
LMC_SC8	337546	↔	LMC_SC7	93939		LMC_SC19	157749	↔	LMC_SC20	21111
LMC_SC9	286128	↔	LMC_SC8	10158		LMC_SC19	163667	↔	LMC_SC20	28803
LMC_SC9	342082	↔	LMC_SC8	52668		LMC_SC19	175567	↔	LMC_SC20	43620
LMC_SC9	349881	↔	LMC_SC8	64709		LMC_SC19	178247	↔	LMC_SC20	47209
LMC_SC9	372259	↔	LMC_SC8	76176		LMC_SC21	187856	↔	LMC_SC5	16
LMC_SC9	372261	↔	LMC_SC8	76179		LMC_SC21	187797	↔	LMC_SC5	19
LMC_SC10	250322	↔	LMC_SC9	45301		LMC_SC21	187853	↔	LMC_SC5	63
LMC_SC10	256258	↔	LMC_SC9	52800		LMC_SC21	193117	↔	LMC_SC5	6197
LMC_SC11	306294	↔	LMC_SC10	35605						

6 Completeness of the Catalog

Cepheids belong to brighter objects among stars in the OGLE photometric databases. With large amplitude of light variations they are relatively easy to detect. Therefore, one can expect that completeness of our Catalog is high.

Completeness of the Catalog can be estimated based on comparison of number of objects detected in the overlapping regions between the neighboring fields. 23 such regions exist between our fields (Fig. 1) allowing to perform 46 tests of pairing objects from a given and adjacent fields. We analyzed full sample of our candidates including detected double-mode Cepheids to increase statistic. In total 217 objects from our full list (Table 3 plus double-mode Cepheid sample) should be paired with counterparts in the overlapping field. We found counterparts in 210 cases which yields the completeness of our sample equal to 96.8%. Thus, our tests indicate that the completeness of our Catalog is indeed very high – practically all Cepheids from the observed fields have been detected.

The completeness is very likely to be even higher. The regions at the field edge are biased in general by smaller number of observations due to imperfections in telescope pointing. Because one of conditions which a star had to fulfill to be searched for variability was 50 observations, this could lead to omission of some objects. Indeed, counterparts of four from our seven unpaired objects had a number of observations smaller than requested and they were not searched for variability at all. We easily detected them as Cepheids when this condition was removed. Two of the remaining objects were missed because of severe blending with other bright stars leading to very noisy light curves. The last unpaired object was a small amplitude, almost sinusoidal shape variable and its counterpart was misclassified as an ellipsoidal variable star.

Comparison of Cepheids from overlapping fields does not take into account completeness of detection of stars by the OGLE data pipeline. It can be derived with artificial star tests. Although such tests have not been performed yet for our LMC fields we can estimate it based on results of tests for the SMC fields with similar stellar density (Udalski *et al.* 1998b). For objects as bright as Cepheids it was found to be larger than 99%. Thus, we may conclude that the total completeness of our Catalog is $>96\%$.

7 Discussion

The OGLE Catalog of Cepheids in the LMC provides an unique, statistically complete sample of these stars ideal for analyzing their properties. The distribution of objects in the LMC is shown in Fig. 1. Dots indicate positions of objects within observed fields. One can easily notice that the distribution is not uniform within the galaxy. Large fraction of objects is located in the south-eastern part of the LMC: in the fields LMC_SC16, LMC_SC17 and LMC_SC18. This region must contain many younger stars and therefore Cepheids are more numerous there than in other regions of the LMC. To make comparison more quantitative Table 5 lists for each field number of objects from the Catalog, number of all stellar objects detected in the field and number of stars brighter than $I_0 = 17.5$ mag (approximately the limit of brightness of classical Cepheids in the LMC).

T a b l e 5

Number of Cepheids and stars in the LMC fields.

Field	N_{Cep}	N_{tot}	$N_{I_0<17.5}$
LMC_SC1	51	341528	27886
LMC_SC2	78	420043	31920
LMC_SC3	58	446233	34541
LMC_SC4	91	482991	37766
LMC_SC5	75	457988	37658
LMC_SC6	84	470171	38366
LMC_SC7	87	473469	39794
LMC_SC8	87	364573	35740
LMC_SC9	56	397307	28661
LMC_SC10	39	292812	26460
LMC_SC11	37	355750	24821
LMC_SC12	19	215267	18562
LMC_SC13	50	273347	20734
LMC_SC14	50	264828	21195
LMC_SC15	48	223749	16125
LMC_SC16	145	269429	25061
LMC_SC17	154	239856	19851
LMC_SC18	91	212219	16783
LMC_SC19	43	195590	15181
LMC_SC20	49	209803	14116
LMC_SC21	43	198314	14898

It should be also noted that positions of many Cepheids coincide with

areas of star clusters and it is very likely that many of them are star cluster members. In the next paper of the series we will provide a full list of Cepheids in the LMC clusters.

The Catalog provides ideal data for studying the Period–Luminosity and Period–Luminosity–Color relations of classical Cepheids – one of the most important features of these stars. Detailed analysis of the $P-L$ and $P-L-C$ relations based on these data was presented in a separate paper (Udalski *et al.* 1999c).

Fig. 4 shows the color-magnitude diagram (CMD) of subfield 2 area of the LMC_SC3 field corrected for the mean $E(B-V)=0.120$ reddening in this direction (Table 2). Field stars from this field are plotted by tiny dots. Larger dots indicate positions of classical Cepheids while open circles positions of the remaining stars from our Catalog.

Based on location of stars in the CMD and $P-L$ W_I-index diagram (Fig. 2) we may draw some conclusions on the objects classified as BR and FA *i.e.*, brighter or fainter than FO and FU mode classical Cepheids. Brighter objects (BR) are usually classical Cepheids, unresolved blends with other star what shifts their magnitudes and colors and changes shape of the light curve. We do not find among them any promising candidate for second overtone mode classical Cepheid contrary to the SMC where large sample of such stars was found (Udalski *et al.* 1999b).

Among fainter objects two main classes can be distinguished. First one consists of Population II Cepheids which are about 2 mag fainter than classical Cepheids. They form a clear sequence below the $P-L$ relation of classical FU mode Cepheids (Fig. 2). The second group (about sixty objects) contains stars with period in the range of $0.8<\log P<1.8$ and the mean $W_I \approx 15.9$ mag. These objects are typically the red giant branch stars and they do not form any noticeable $P-L$ relation. Although their light curves resemble those of pulsating stars, it may happen that their real variability is not related to pulsations. A few shortest period stars from the FA group might be longer period RR Lyr stars located in front of the LMC (distance modulus about $1-1.5$ mag smaller than that of the LMC). A few objects located in Fig. 2 close to the boundary of FU mode Cepheids are highly reddened FU Cepheids or Cepheids blended with blue stars.

Fig. 5 presents the distribution of color indices $V-I$ of classical FU and FO mode Cepheids. The mean $(V-I)_0$ color and its dispersion are equal to $(0.604, 0.08)$ and $(0.509, 0.08)$ for the FU and FO mode Cepheids in the LMC, respectively. The distribution can be well approximated with a Gaussian but an excess of red objects is clearly seen for both types of

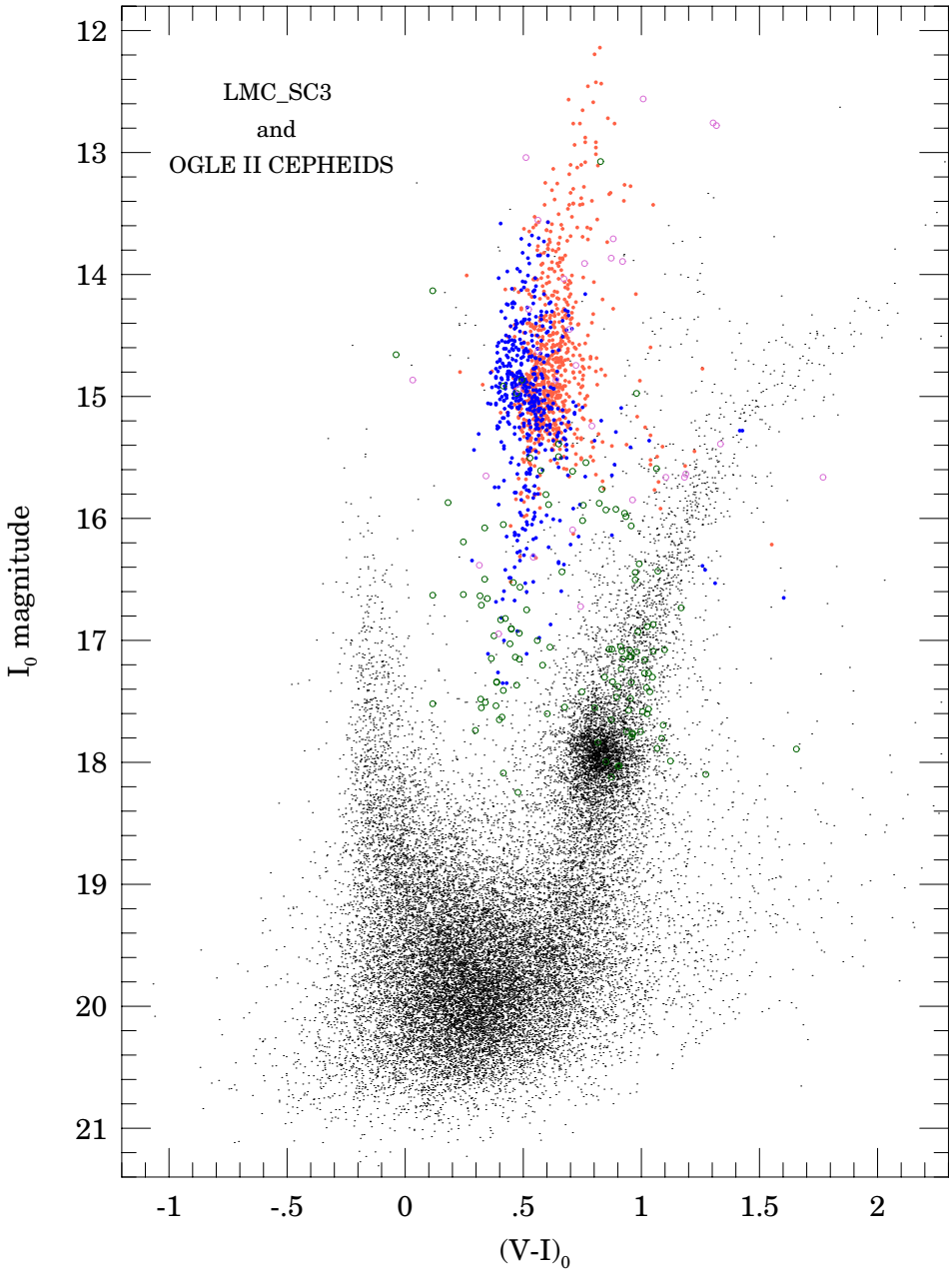

Fig. 4. Color-magnitude diagram of subfield 2 of the LMC_SC3 field. Only about 20% of field stars are plotted by tiny dots. Larger dots show positions of FO and FU classical Cepheids (dark and light dots, respectively). Dark and light open circles mark positions of objects from the Catalog classified as FA and BR, respectively.

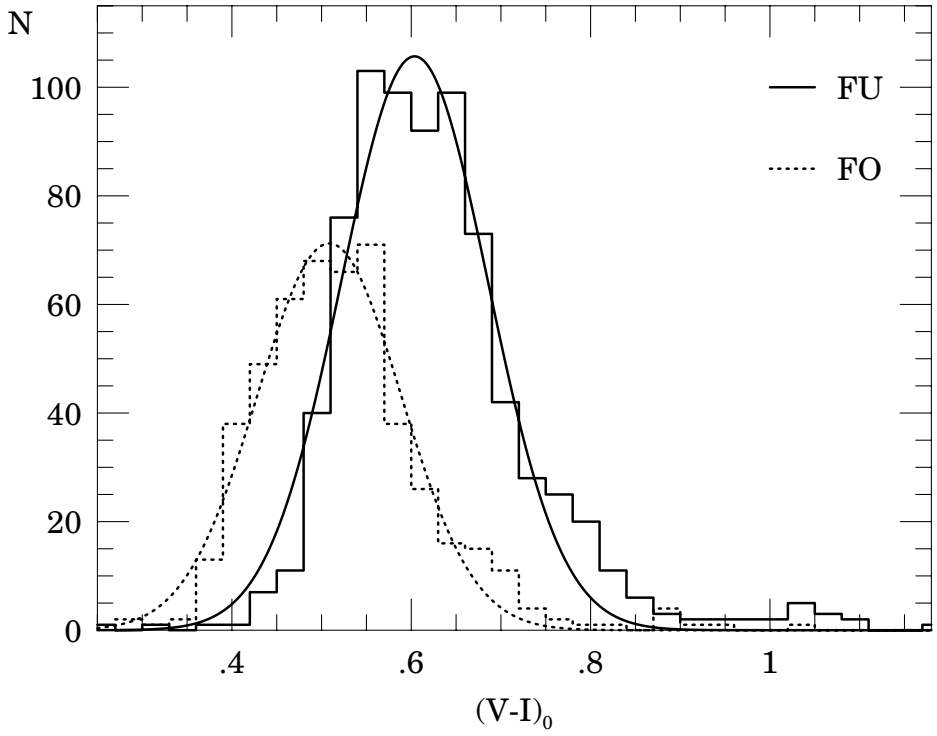

Fig. 5. Histograms of $(V-I)_0$ color distribution of single-mode Cepheids in the LMC. Solid line represents distribution of fundamental mode pulsators, dotted line – first overtone objects. The bins are 0.03 mag wide.

Cepheids. It is partially caused by Cepheids reddened more than the mean correction applied. This effect is also seen in Fig. 4 for field stars – the red clump is slightly elongated in the direction of reddening. Another reason of excess of red objects is bending of the instability strip in the CMD diagram for brighter (redder) objects.

Fig. 6 shows distribution of periods of FU and FO mode classical Cepheids in the LMC. Typical period of the FU mode Cepheid in the LMC is about 3.2 days while for the FO mode objects 2.1 days. The fundamental mode Cepheid period distribution has a long tail toward long period objects and the number of Cepheids with period shorter than 2.3 days falls rapidly to zero. The longest period of the FO mode Cepheids is about 6.4 days while the shortest periods are of about 0.4 day.

Different distribution of periods and different metallicity of Cepheids in the LMC and SMC ([Fe/H] $= -0.3$ dex, and -0.7 dex for the LMC and

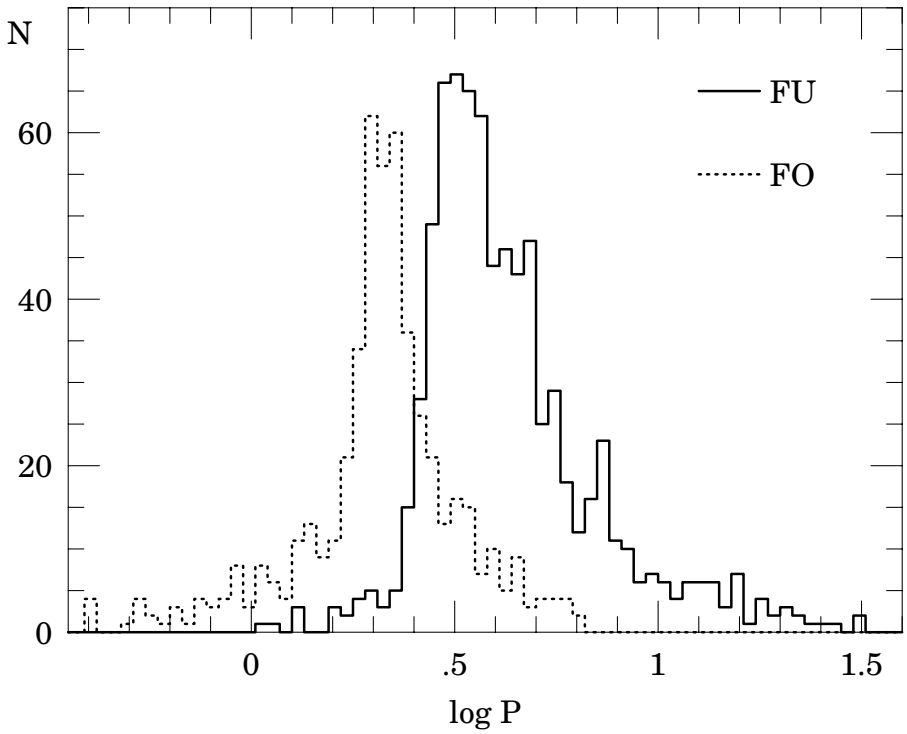

Fig. 6. Histograms of $\log P$ distribution of single-mode Cepheids in the LMC. Solid line represents distribution of fundamental mode pulsators, dotted line – first overtone objects. The bins are 0.03 wide in $\log P$.

SMC, respectively, Luck *et al.* 1998) result in somewhat different diagrams of Fourier parameters of light curve decomposition (*cf.* Fig. 3 and Fig. 2 of Udalski *et al.* 1999a). Detailed analysis of these diagrams may provide information on dependence of the shape of Cepheid light curve on metallicity.

Among many individual objects which show full variety of Cepheid behaviors (*e.g.*, many "bump" Cepheids) three objects require a special attention. They are the binary, eclipsing systems including Cepheid as a component: LMC_SC7 239698, LMC_SC21 40876 and LMC_SC16 119952. The first two of these objects were already found by the MACHO group (Welch *et al.* 1999). Such systems are very important because their precise photometry and spectroscopy can provide accurate information on sizes and masses of the components. LMC_SC7 239698 is a Population II Cepheid while the remaining stars are classical Cepheids. LMC_SC21 40876 is a FU mode pulsator. LMC_SC16 119952 pulsates in the FO mode.

Fig. 7 shows the light curves of these three Cepheids. In the left panel the light curve phased with the Cepheid period is presented. In the right panel the light curve with subtracted Cepheid variability (by approximation of its light curve with Fourier series) is displayed. For LMC_SC7 239698 and LMC_SC21 40876 observations are folded with the eclipsing period. It should be noted that the eclipsing periods are very preliminary because the binary systems containing Cepheids are very wide and only 2–3 eclipses were observed during the entire period of the OGLE observations. They will be refined after the next observing seasons. For LMC_SC16 119952 only one clear eclipse was observed, thus we present its light curve in day units along the ordinate.

We also draw attention to another interesting object – LMC_SC6 330185. Its variations are consistent with a sum of light of two Cepheids either being optical blend or physically related. Both components are the FO mode pulsators with periods 2.48092 and 1.96376 days. This object was already presented by the MACHO group (Alcock *et al.* 1995).

The Catalog of Cepheids from the LMC is available now to the astronomical community from the OGLE Internet archive:

http://www.astrouw.edu.pl/~ftp/ogle
ftp://sirius.astrouw.edu.pl/ogle/ogle2/var_stars/lmc/cep/catalog/

or its US mirror

http://www.astro.princeton.edu/~ogle
ftp://astro.princeton.edu/ogle/ogle2/var_stars/lmc/cep/catalog/

The data include the mean photometry, individual BVI observations of all objects and finding charts. We plan to update the Catalog in the future when more observations are collected. We would also appreciate information on any errors in the Catalog which are unavoidable in so large data set.

Acknowledgements. We would like to thank Prof. Bohdan Paczyński for many discussions and important suggestions. We thank Dr. K. Z. Stanek for valuable comments and remarks on the paper. We are also grateful to Dr. D. Welch for pointing out wrong period of LMC_SC16 119952 eclipsing Cepheid in the original version of the paper. The paper was partly supported by the Polish KBN grants 2P03D00814 to A. Udalski and 2P03D00916 to M. Szymański. Partial support for the OGLE project was provided with the NSF grant AST-9530478 and AST-9820314 to B. Paczyński. We acknowledge usage of The Digitized Sky Survey which was produced at the Space

Telescope Science Institute based on photographic data obtained using The UK Schmidt Telescope, operated by the Royal Observatory Edinburgh.

REFERENCES

Alcock, C. *et al.* 1995, *Astron. J.*, **109**, 1652.
Alcock, C. *et al.* 1999, *Astrophys. J.*, **511**, 185.
Bauer, F. *et al.* 1999, *Astron. Astrophys.*, **348**, 175.
Bica, E., Geisler, D., Dottori, H., Clariá, J.J., Piatti, A.E., and Santos Jr, J.F.C. 1998, *Astron. J.*, **116**, 723.
Harris, J., Zaritsky, D., and Thompson, I. 1997, *Astron. J.*, **114**, 1933.
Leavitt, H.S. 1912, *Harvard Cir.*, 173.
Lee, M.G. 1995, *JKAS*, **28**, 177.
Luck, R.E, Moffett, T.J., Barnes, T.G., and Gieren, W.P. 1998, *Astron. J.*, **115**, 605.
Madore, B.F., and Freedman, W.L. 1991, *P.A.S.P.*, **103**, 933.
Sasselov, D., *et al.* 1997, *Astron. Astrophys.*, **324**, 471.
Schlegel, D.J., Finkbeiner, D.P., and Davis, M. 1998, *Astrophys. J.*, **500**, 525.
Schwarzenberg-Czerny, A. 1989, *MNRAS*, **241**, 153.
Stanek, K.Z. 1996, *Astrophys. J. Letters*, **460**, L37.
Udalski, A., Kubiak, M., and Szymański, M. 1997, *Acta Astron.*, **47**, 319.
Udalski, A. 1998a, *Acta Astron.*, **48**, 113.
Udalski, A. 1998b, *Acta Astron.*, **48**, 383.
Udalski, A., Szymański, M., Kubiak, M., Pietrzyński, G., Woźniak, P., and Żebruń, K. 1998a, *Acta Astron.*, **48**, 1.
Udalski, A., Szymański, M., Kubiak, M.,Pietrzyński, G., Woźniak, P., and Żebruń, K. 1998b, *Acta Astron.*, **48**, 147.
Udalski, A., Pietrzyński, G., Woźniak, P., Szymański, M., Kubiak, M., and Żebruń, K. 1998c, *Astrophys. J. Letters*, **509**, L25.
Udalski, A., Soszyński, I., Szymański, M., Kubiak, M., Pietrzyński, G., Woźniak, P., and Żebruń, K. 1999a, *Acta Astron.*, **49**, 1.
Udalski, A., Soszyński, I., Szymański, M., Kubiak, M., Pietrzyński, G., Woźniak, P., and Żebruń, K. 1999b, *Acta Astron.*, **49**, 45.
Udalski, A., Szymański, M., Kubiak, M., Pietrzyński, G., Soszyński, I., Woźniak, P., and Żebruń, K. 1999c, *Acta Astron.*, **49**, 201.
Walker, A.R. 1993, *Astron. J.*, **105**, 527.
Welch, D.L. *et al.* 1999, in Proceedings of IAU Symposium 190, "New Views of the Magellanic Clouds"; (astro-ph/9901282).

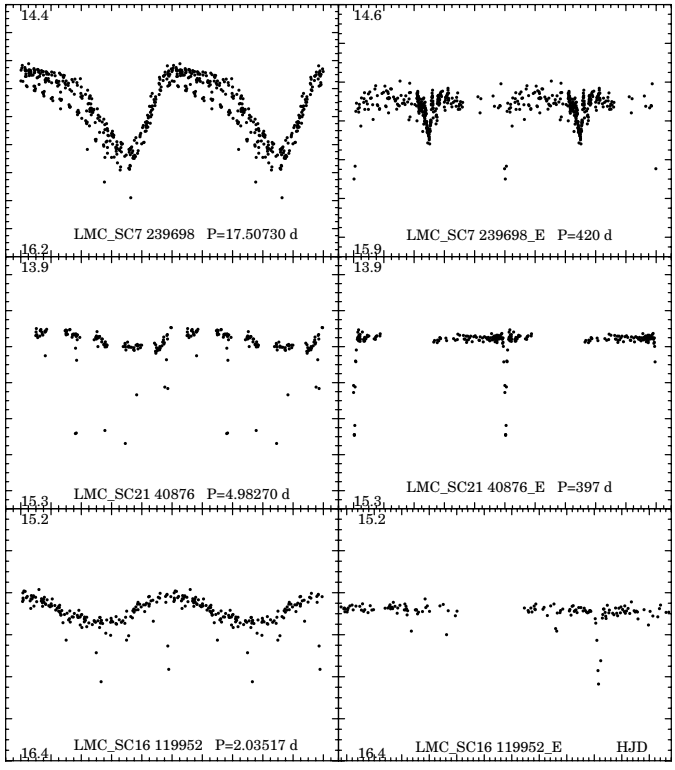

Fig. 7. Light curves of three eclipsing binary systems with Cepheid component. In the left panel observations are folded with the Cepheid period. In the right panel eclipsing light curve is shown after subtracting the brightness of Cepheid component. Abscissa is the *I*-band magnitude and the ordinate – phase with 0.0 value corresponding to maximum brightness in the left panels and middle of deeper eclipse in two upper right panels. For LMC_SC16 119952 the ordinate of the right panel is in HJD with larger ticks separated by 50 days and the most right large tick equal to HJD = 2451300.

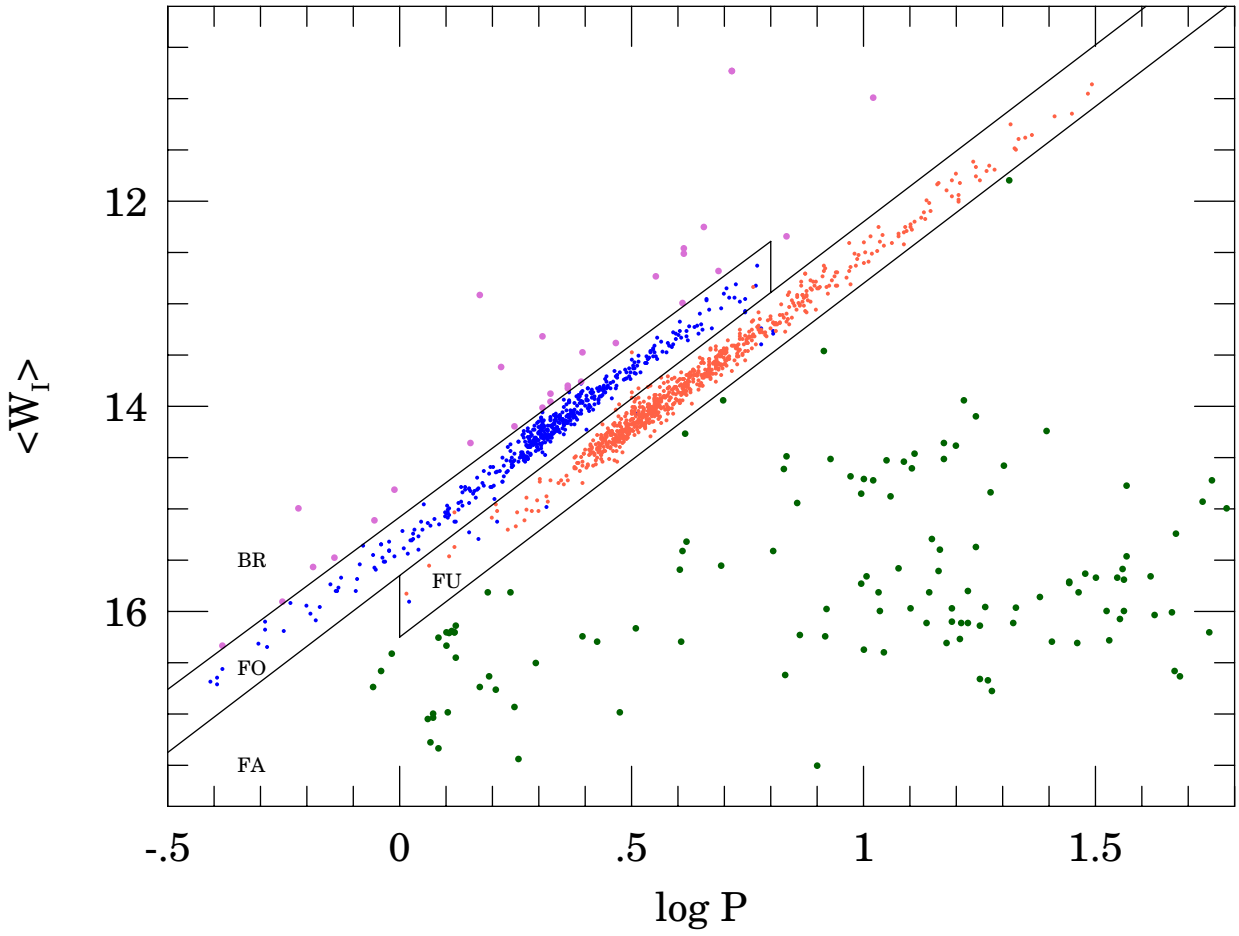
12
14
16
<W_I>
BR
FO
FA
FU
-.5
0
.5
1
1.5
log P

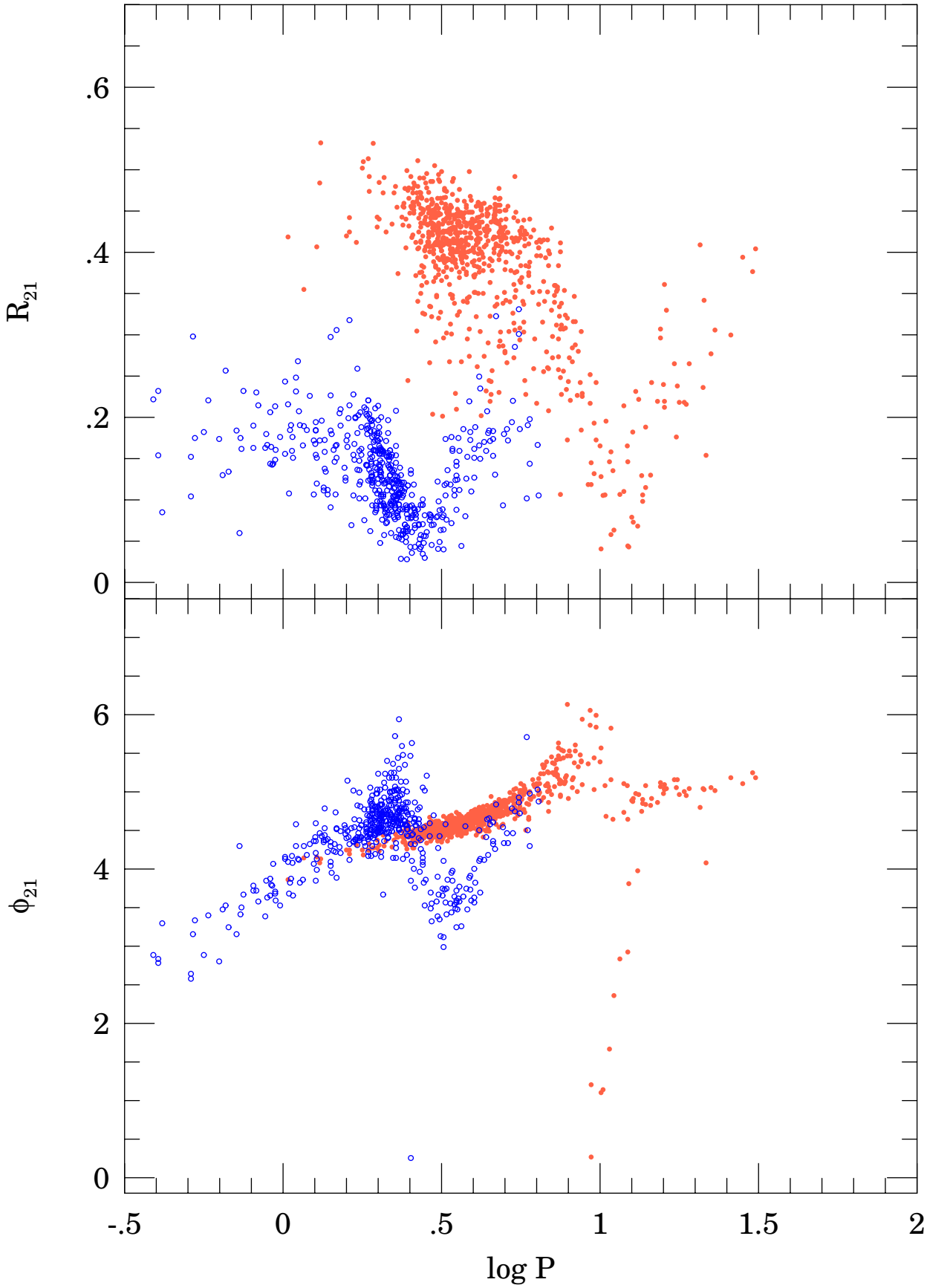
.6
.4
.2
0
R_{21}
6
4
2
0
ϕ_{21}
-.5
0
.5
1
1.5
2
log P

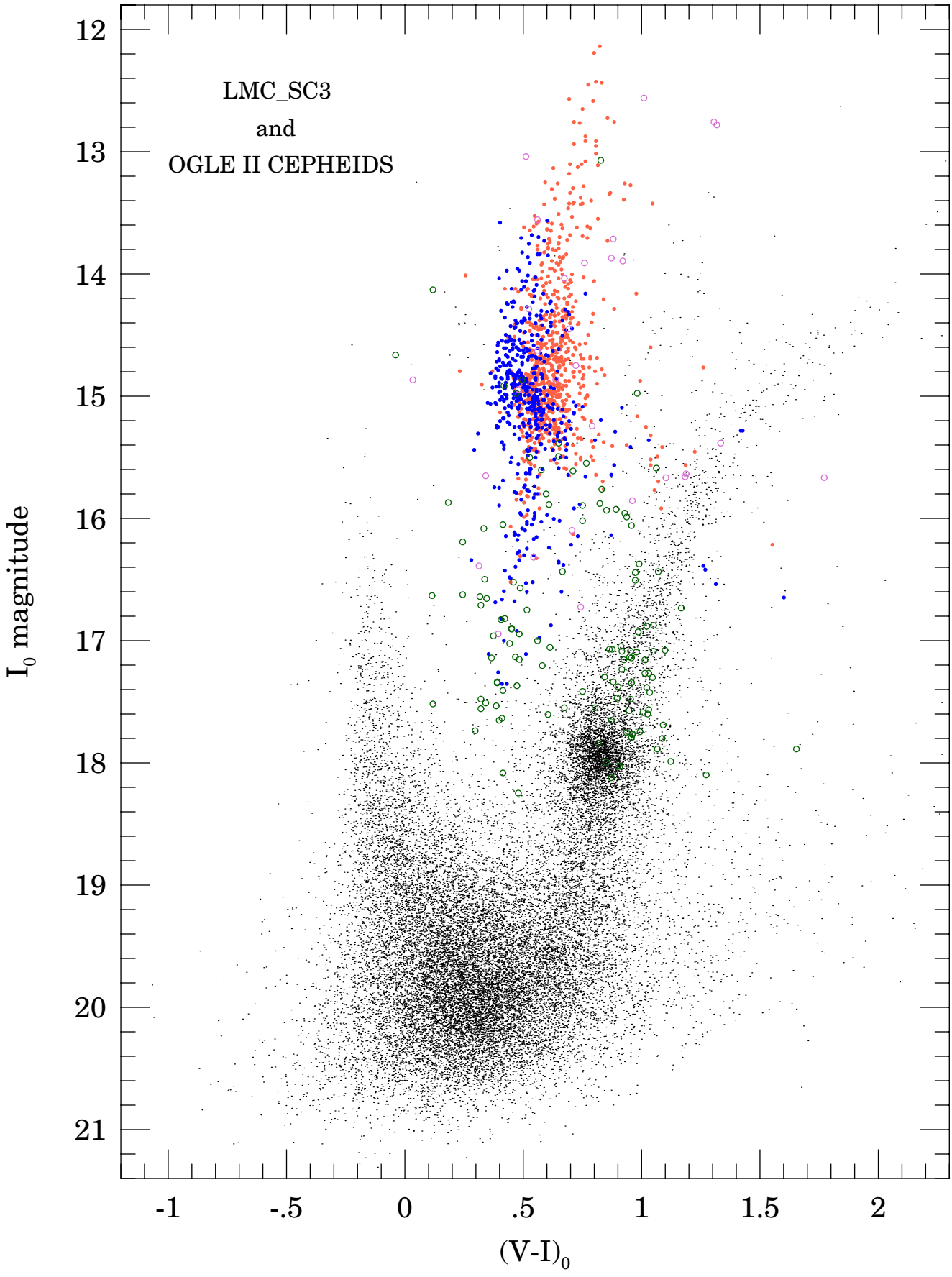
LMC_SC3
and
OGLE II CEPHEIDS
12
13
14
15
16
17
18
19
20
21
I0 magnitude
-1
-.5
0
.5
1
1.5
2
(V-I)0

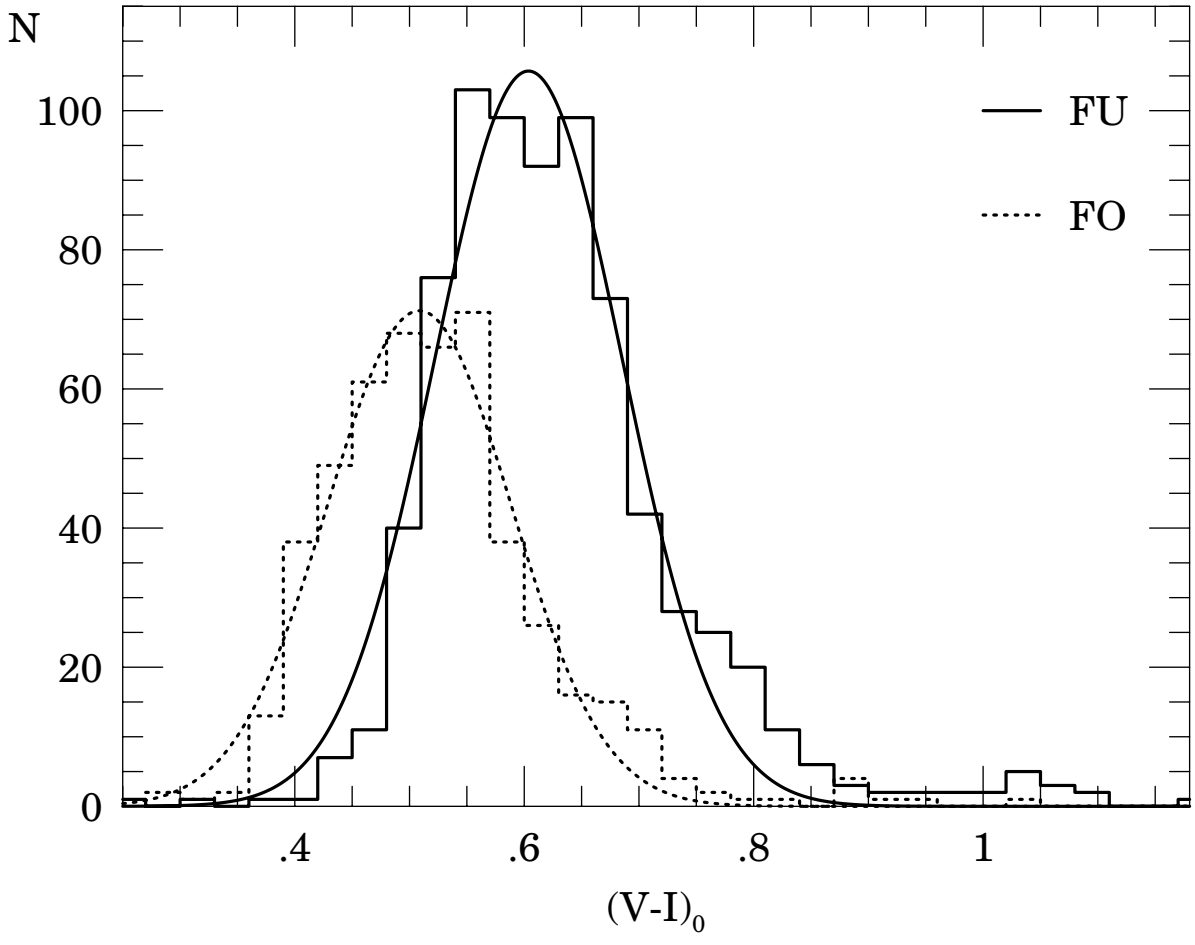
N
100
80
60
40
20
0
.4
.6
.8
1
(V-I)0
FU
FO

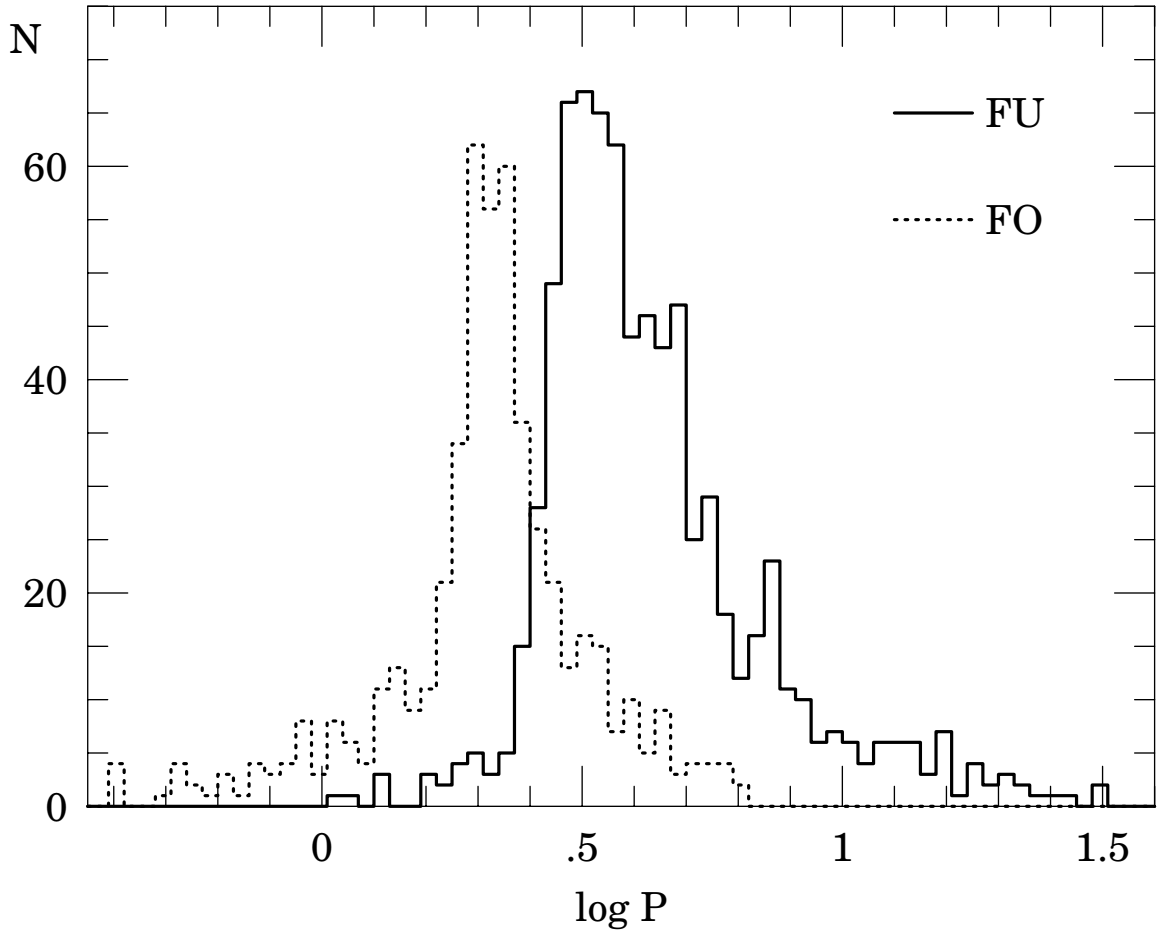
N
60
40
20
0
FU
FO
0
.5
1
1.5
log P

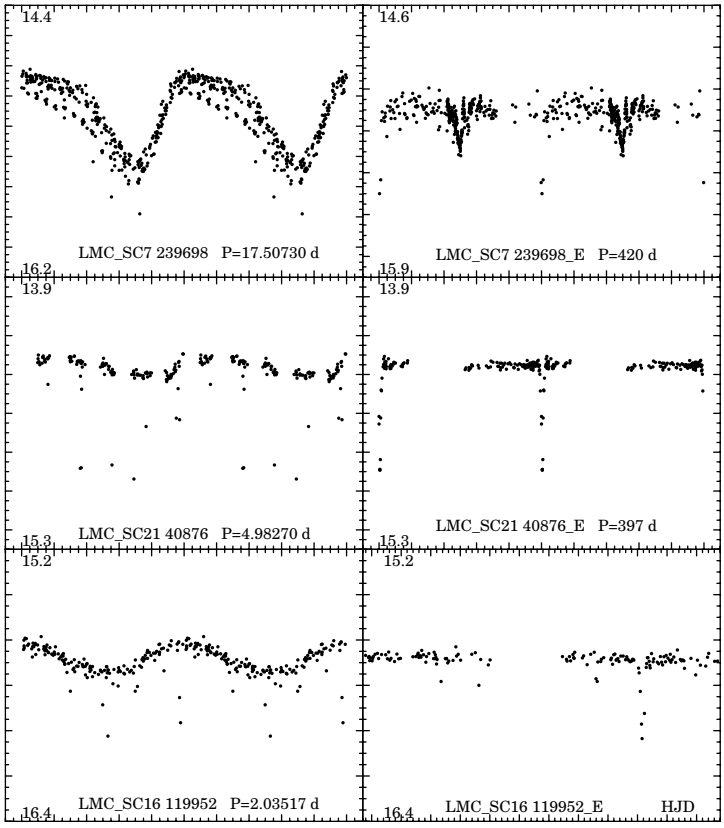
14.4
LMC_SC7 239698 P=17.50730 d
16.2
14.6
LMC_SC7 239698_E P=420 d
15.9
13.9
LMC_SC21 40876 P=4.98270 d
15.3
13.9
LMC_SC21 40876_E P=397 d
15.3
15.2
LMC_SC16 119952 P=2.03517 d
16.4
15.2
LMC_SC16 119952_E
16.4
HJD